

# Stability of geocell-reinforced soil

J. N. Mandal\*<sup>†</sup> and P. Gupta<sup>‡</sup>

<sup>†</sup>*Civil Engineering Department, IIT, Powai, Bombay-400 076, India*

<sup>‡</sup>*Tata Consultant Engineer, India*

*Received 25 November 1992; accepted 22 March 1993*

Engineers often experience difficulties in starting any construction work on soft clay because there is no hard strata at a depth of 15 m. The application of a geocell structure provides a comparatively harder stratum at the top of the soft subgrade. Therefore, experimental investigations have been carried out on the stability of a geocell-reinforced soft soil structure, to evaluate the effect of the geocell configuration (i.e. geocell opening size, height) on the bearing capacity and the failure settlement of a two-layer system. The laboratory model tests for ultimate bearing capacity of marine clay overlain by a sand layer with and without the geocell are performed to study load-settlement characteristics and the increase of bearing capacity and reduction of settlement. The model foundation used is just strip footing on the surface. The actual behaviour of the geocell structure under different external loading conditions has been revealed in these studies. It has been observed that load-settlement characteristics are improved owing to the use of geocell reinforcement. In addition, an improved bearing capacity factor has been suggested on the basis of the experimental results.

**Keywords:** geocell reinforcement; soft soils; stability

Geosynthetics are being increasingly used in geotechnical engineering activities. These reinforcement materials are used as a practical means of solving various construction problems, e.g. in dams, foundations, roads, erosion control, retaining structures, etc. By using geotextiles as a reinforcement, the total cost of the project may be reduced by a considerable amount. The pioneering work on horizontal layers of geotextiles has been documented by several investigators<sup>1-9</sup>.

Geotextiles derive their strength from a substantial amount of settlement of the structure which, though acceptable in unpaved roads, may not be suitable for paved roads or any kind of structure where large settlement causes severe damage to the structure. This necessitates the use of high-modulus geotextiles or any confinement technique like geocell or geoweb. In a country like India, the latter is the best alternative solution for problems where allowable settlement is very low.

The geocell confinement system not only increases the load-bearing capacity of the soil but also substantially reduces the settlement. This is achieved by the confinement of the failure wedges which would be developed in an unreinforced soil from laterally and outward displacement. The lateral movement and shear failure are resisted by both the tensile hoop strength of the cell walls and the passive resistance of the full adjacent cells. In addition, the frictional interlock between the infill material and the cell walls allows the load to be distributed or shared with adjacent cells. Garidel and Morel<sup>10</sup> conducted punching tests using a rigid circular plate on an armater geocell in silty subsoils. They carried out both

small- and large-displacement tests and found that, for large displacements, there was a vertical shearing of the sand and the deformed shape of fill material was almost the same as subgrade material.

Khay and Perrier<sup>11</sup> investigated the suitability and mechanical behaviour of armater geocells in granular subgrade material. Geocells used had an  $a/b$  ( $a$  = geocell size and  $b$  = geocell height) ratio of 0.5 with varying  $b$  of 10, 15 and 20 cm. The geocell structure showed considerable trafficability enhancement. The settlement of the geocell structure was markedly low, indicating the slab effect of such structures.

Kazerani and Jamnejad<sup>12</sup> carried out some tests on geocell-reinforced soft subgrade material which was simulated by using blocks of medium-density polystyrene. Poorly graded and well-graded soils were used separately as a base soil. Both cyclic load and static load were applied. A considerable improvement in the mechanical properties of the poorly graded granular fills was found by preventing the degradation of the fill particles.

Basset<sup>13</sup> has also implied that, in laboratory studies, a three-dimensional geocell proved about five times stiffer in bending than the same weight of two-dimensional sheets of similar grid materials with sand placed on top to the same depth as the geocell.

Mhasikar and Mandal<sup>14</sup> have investigated the efficacy of the geocell structure on a soft clay subgrade. The geocells were filled by sand. Experimental and finite element (i.e. AWSYS, a general-purpose finite element package) procedures have been used to study the improvement in stiffness. Paul<sup>15</sup> has also reported on the use of a Tensar grid-formed geocell mattress in Scotland.

Shimizu and Inuc<sup>16</sup> carried out model tests to investi-

\*Correspondence to Professor J. N. Mandal

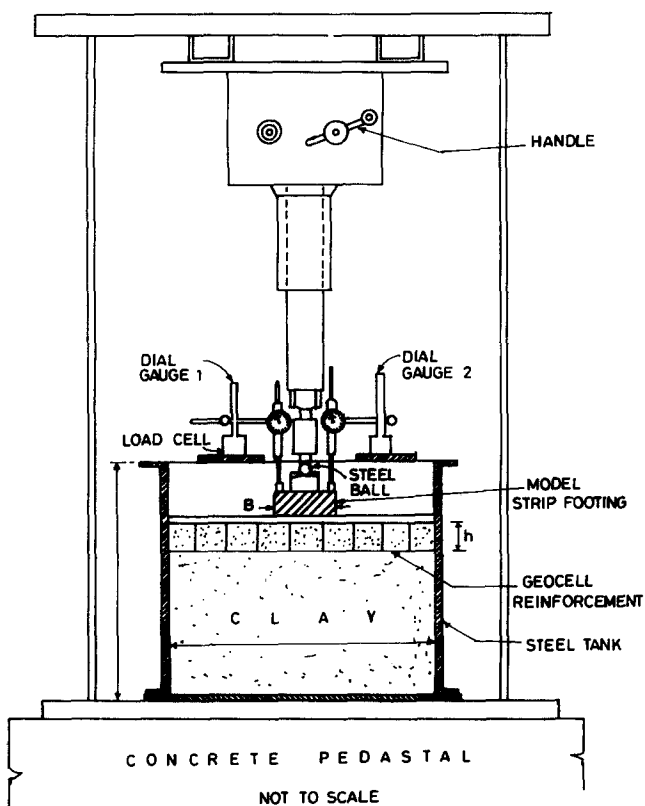


Figure 1 Schematic diagram of test set-up

gate the resistance of paper/cardboard cells of a geocell structure embedded in loose sand.

Bush *et al.*<sup>17</sup> reported on the use of a geocell foundation mattress. The cells were fabricated directly on a soft foundation soil from polymer grid reinforcement and then filled with granular material resulting in a structure 1 m deep.

In the present paper, tests have been conducted to study the variation of bearing capacity with geocell size at a constant value of geocell height. An improved bearing capacity factor has been suggested on the basis of the experimental results.

### Model test arrangement

The model tests were conducted in a rectangular tank 61 cm long, 31 cm wide and 40 cm deep. A 20.5 cm long and 7.3 cm wide rigid, cast-iron strip footing spanned the width of the tank. The footing was composed of three segments loaded as a unit so as to produce a uniform distribution of applied pressure on the surface. The vertical loads were applied from a hand-operated jack system through a load cell of 1000 kg capacity. The deformations were read with two dial gauges placed at the two ends of the footing. The average readings of deformations were taken into account for the differential deformations. A schematic diagram of the test set-up is shown in Figure 1. The loads were applied in small increments and the resulting deformations were noted so that the entire load settlement curve to failure was obtained. The load was recorded by an electronic recorder. The geocells used in the experiment were made up of Tata Mills, non-woven polypropylene type 425A, whose properties are given in Table 1. These geocells were constructed by

Table 1 Properties of geotextile 425a

1	Maximum width (cm)	137
2	Fibre	Polypropylene
3	Wt per m <sup>2</sup> (± 10%) (g)	300
4	Water permeability (L m <sup>-2</sup> s <sup>-1</sup> ) at 10 cm water head	74
5	Specific gravity	0.907
6	Mean pore size	130
7	Breaking load (kg) (5 cm × 20 cm strip)	
	Lengthwise (warp)	50
	Widthwise (weft)	40
8	Elongation at break (%)	
	Lengthwise	50
	Widthwise	70
9	Thickness (mm) (+ 10%)	2.3
10	Bursting strength (kPa)	78
11	Air permeability (m <sup>3</sup> h <sup>-1</sup> m <sup>-2</sup> )	1300

Table 2 Properties of marine clay

Liquid limit (%)	73.8
Plastic limit (%)	41.0
Plasticity index (%)	32.8
Shrinkage limit (%)	17.0
Specific gravity	2.72
Textural classification	
Gravel (%)	0
Sand (%)	4.0
Silt (%)	34.0
Clay (%)	62.0
IS classification	OH or mh
Engineering properties:	
Modified Proctor maximum density (kg m <sup>-3</sup> )	1315
Optimum moisture content (%)	31
Cohesion (kPa)	20
Y <sub>bulk</sub> (g cm <sup>-3</sup> )	1.67
Y <sub>dry</sub> (G cm <sup>-3</sup> )	1.08
e (void ratio)	1.5
S (degree of saturation) (%)	92
n (porosity)	0.6
Water content (%)	52

pasting strips of geotextiles alternately depending on the desired geocell opening size. The adhesive used for pasting was Alkamelt-20, a heat-bonded adhesive manufactured by ICA (Industrial Chemical Association) Geocells. The strength of the joint was 1700 N m<sup>-1</sup>.

### Preparation of test sample

Air-dry pulverized soil (marine clay) was compacted to prepare a soft subgrade material. The properties of the marine clay are given in Table 2.

The marine clay was compacted in five layers each of 5 cm thickness. The amount of air-dry soil needed was calculated on the basis of a dry density of 1.08 g cm<sup>-3</sup> and a moisture content of 50%. The water added amounted to 39% (taking 11% as the hygroscopic moisture content for marine clay). For compacting the soil in a rectangular tank, a base plate of 15 cm × 15 cm was used. The modified Proctor hammer was placed centrally on the plate and three blows were imparted in one position to attain a subgrade strength of 20 kPa. A total of 24 blows per layer were required to attain the desired compaction.

A layer of sand was placed at the bottom of the tank and three sides of the tank were covered by Gunny bags for drainage. After placing a filter paper on the bottom sand layer, the compacted subgrade was prepared and

**Table 3** Properties of Mumbra sand

Maximum density ( $\text{g cm}^{-3}$ )	1.81
Minimum density ( $\text{g cm}^{-3}$ )	1.605
Uniformity coefficient	4.6
Relatively density (%):	
$D_{50}$	0.42
$D_{10}$	0.165
Density of sand ( $\text{g cm}^{-3}$ )	1.6869

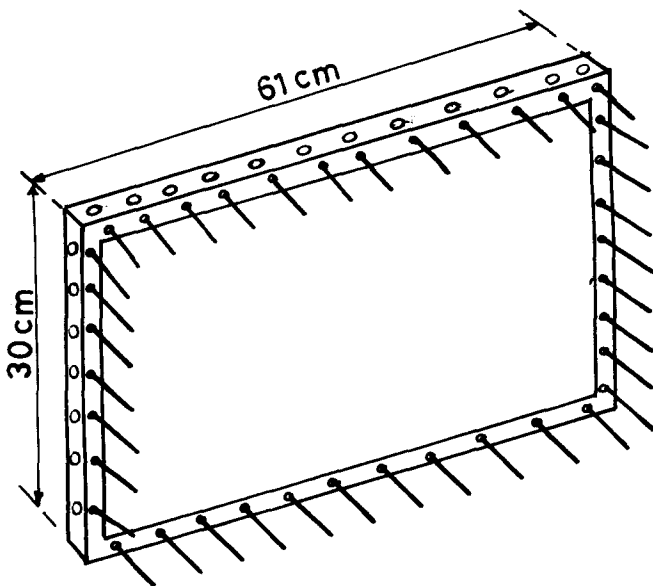
**Table 4** Properties of geocell structure

No.	Title	Values
1	Expanded dimension	$60 \times 30 \times 7.3 \text{ cm}^3$
2	Collapsed dimension	$7.5 \times 5 \times 7.3 \text{ cm}^3$
3	Panel thickness nominal	0.363 cm
4	Weight	
5	Cell area	$26.6 \text{ cm}^2$
6	Cell seam node pitch	7.2 cm
7	Glue/seam	1
8	Seam tensile peel strength	$1700 \text{ N m}^{-1}$
9	Installation temperature	$24\text{--}30^\circ\text{C}$
10	Material of geotextiles	Polypropylene
11	Colour	White
12	Chemical resistance	Medium
13	Frictional efficiency ( $E_f$ )	0.74

**Table 5** Test set-up

No.	Description
1	Strip footing resting on soft marine clay
2	Strip footing resting on sand layer underlain by soft marine clay with $h/B = 0.75, 1.0, 1.25, 1.5$ and $1.7$
3	Strip footing resting on geocell-reinforced sand underlain by soft marine clay; geocell size $a = 0.024 \text{ m}$ , $h/B = 0.75, 1.0, 1.25$ and $1.5$
4	Strip footing resting on geocell-reinforced sand layer underlain by soft marine clay; geocell size $a = 0.032 \text{ m}$ , $h/B = 0.75, 1.0, 1.25$ and $1.5$
5	Strip footing resting on geocell-reinforced sand layer underlain by soft marine clay; geocell size $a = 0.04 \text{ m}$ , $h/B = 0.75, 1.0, 1.25$ and $1.5$

$h$  = thickness of reinforced or unreinforced sand layer,  $B$  = footing width and  $a$  = geocell opening size


**Figure 2** Special arrangement for expanding geocell

again covered with a filter paper. A sand layer was kept on that filter paper for 3 days during the saturation period to avoid the formation of slush.

### Test procedure

After  $3\frac{1}{2}$  days of saturation, which helped to obtain about 92% of saturation in the subgrade, the tank was placed centrally at the bottom of the loading frame. Now, in the unreinforced case, a calculated amount of sand (calculated on the basis of a relative density,  $D_r$ , of 60% and a dry density,  $\gamma_d$ , of  $1.6869 \text{ g cm}^{-3}$  was accommodated in the known volume of the tank, which depended on the  $h/B$  ratio. The properties of sand are listed in Table 3.

Tamping was done with a cast-iron rod of weight 140 g, and which required 15 blows from a height of 10 cm to attain the required strength. In the reinforced case, the volume of sand required was calculated by deducting the volume of geotextile material used from the volume of the tank. Around 15 blows per cell were applied from a height of 10 cm, with the same cast-iron rod, to attain the relative density of 60%.

The geocell structure was first expanded by an arrangement shown in Figure 2 and then filled with sand. After compaction, this arrangement was removed. The expanded dimension of the geocell structure was the same as that of the tank. The parameters of the geocell structures are given in Table 4.

Two dial gauges were fixed on either side of the centre of the footing to record the footing settlement for each increment of load. The electronic recorder was used for recording the load applied through the load cell. The load was transmitted to the footing through a steel ball placed centrally on the footing.

After setting up the arrangement properly, power was supplied to the electronic recorder. The loading was applied by the hand-operated hydraulic jack for the stress control tests and the amount of load applied was read by the electronic recorder.

The load was applied in steps of 30 kg for the reinforced case and 20 kg for the unreinforced case. For every load step the load was kept constant till the front dial gauges showed a rate of settlement of less than  $1 \text{ mm min}^{-1}$  for the unreinforced case and  $0.5 \text{ mm min}^{-1}$  for the reinforced case. Only elastic settlements were calculated, not consolidation settlements.

Failure was noticed by the sinking of the footing at a very fast rate and difficulties were encountered in maintaining a constant load.

The load-settlement diagrams were drawn to find the improvement factor (IF) at each settlement. The De Beer<sup>18</sup> failure criterion has been used to determine the ultimate bearing capacity and the settlement of failure.

### Results and discussions

A summary of the tests performed is given in Table 5. The tests were performed on subgrade of strength 20 kPa with 60% relative density of backfill.

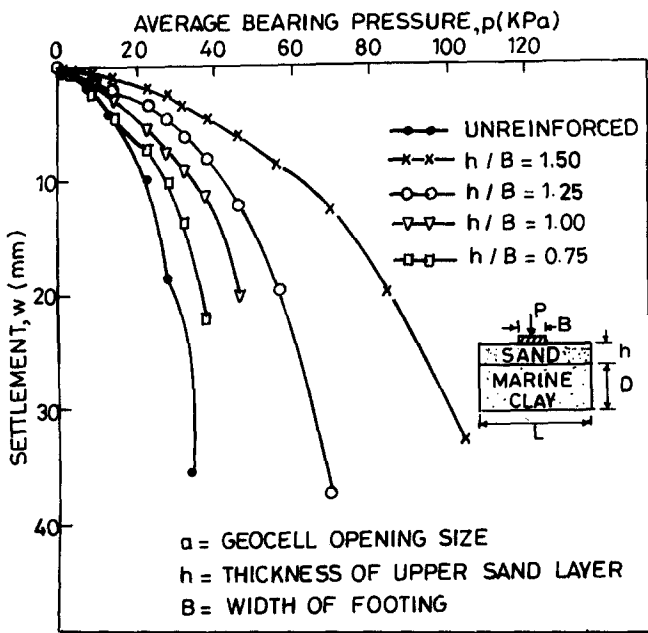


Figure 3 Load-settlement curves of strip footing on unreinforced sand layer over soft marine clay

Load-settlement curves were drawn for each of the experiments. In all of these experiments punching failure was observed. In order to identify the failure clearly, the load-settlement diagrams were drawn in the dimensionless form of  $\ln(p/A\gamma B)$  vs  $\ln(w/B\%)$ , where  $p$  is average bearing pressure.  $A$  is the dimensionless factor given by De Beer<sup>18</sup>.

Figure 3 shows the load settlement curves of the strip footing on unreinforced sand over soft marine clay for varying thicknesses of sand layer.

It can be seen from Figure 3 that, at the initial stage, settlement increases with an increase of pressure but beyond a certain settlement there is a large settlement with a small increment of pressure, which indicates the plastic flow of soil. In the case of clay only this phenomenon starts earlier and, as the thickness of the sand layer increases, the plastic flow is deferred. It should also be noted that the slope of the curve at the initial stage (i.e. initial stiffness) increases with the increased layer thickness. At any settlement, the greater the thickness of the sand layer, the more will be the pressure-carrying capacity. As there is no definite failure point visible in the curve the failure must be due to punching shear. To identify the actual failure parameter De Beer's method<sup>18</sup> has been adopted.

Figure 4 shows the load-settlement curves of the strip footing on both the unreinforced and the geocell-reinforced sand layer over soft marine clay at  $h/B = 1.0$  for three different values of  $a$ , the geocell opening size. From Figure 4 it can be seen that, in the unreinforced case, settlement increases with load and beyond a certain point there is a large settlement caused by a small increment of load. But this behaviour is somewhat different in the reinforced case at the later stage. Initially settlement increases linearly with load and, after a certain point slope of the curve, decreases gradually. Again, beyond a certain point it becomes a straight line. No definite failure point has been indicated and that is why De Beer's method was used to evaluate the settlement parameters.

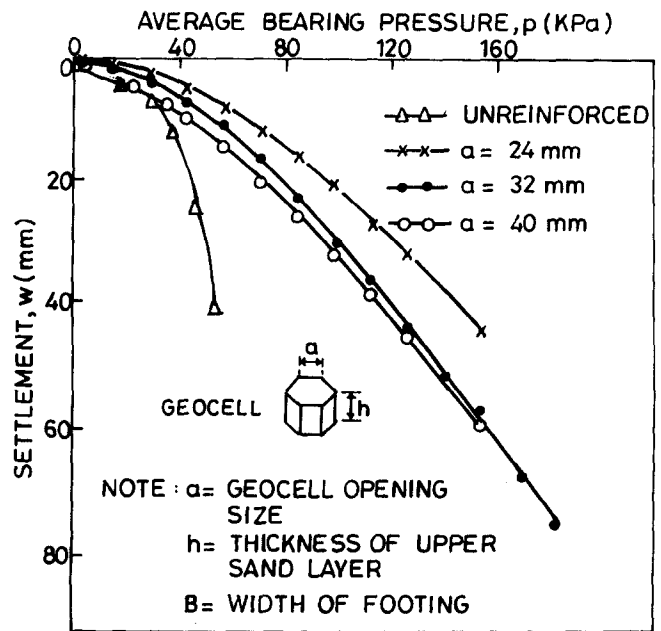


Figure 4 Load-settlement curves of strip footing on unreinforced and geocell-reinforced sand layer over soft marine clay at  $h/B = 1.0$

A glance at the nature of the curves for all three reinforced cases will reveal that they consist of three parts. The initial linear part seems to be due to the initial beam action of the geocell layer at a low settlement ratio of about 5–10%. The middle curve part seems to be due to the mixed beam and membrane action of the geocell walls at a settlement ratio of 10–20%; at a large settlement the tensile strength seems to be contributing to the load-carrying capacity. The final linear part seems to be due to the predominant membrane action of the geocell layer at a large settlement ratio of 20% or more. A conspicuous improvement of sand for the reinforced condition compared with the unreinforced case can be seen in Figure 4. As the failure occurs at large settlement, Figure 4 allows a good comparison of the ultimate bearing capacity at large settlement. The load-settlement curve can be utilized to predict the bearing capacity under both the low-settlement and the large-settlement condition depending on the practical problems. Settlement ratios of 10% and 50% can be taken as the criteria for low-settlement bearing capacity and large-settlement bearing capacity, respectively.

Figure 5 shows the variation of the improvement factor (IF) with settlement ratio ( $s/B$ ) for both the unreinforced and the reinforced case at  $h/B = 1.0$ . It can be seen from Figure 5 that in the unreinforced case the IF increases with settlement ratio initially and beyond a certain settlement. In the reinforced case the IF is much more than that in the unreinforced case. An improved initial stiffness can be inferred. IF remains constant up to a 10% settlement ratio (low-settlement case) in the reinforced case. After that it increases with settlement ratio. The increase of stiffness is greater in the case of the lower geocell opening size. However, at large settlement, there is a marginal improvement for geocell sizes of  $a = 32$  and  $40$  mm. The reason is that if the geocell opening size is more than at large settlement ratio, the size of the geocell does not affect the improvement, because at large settlement the membrane action is assumed to be predominant and sizes become immaterial.

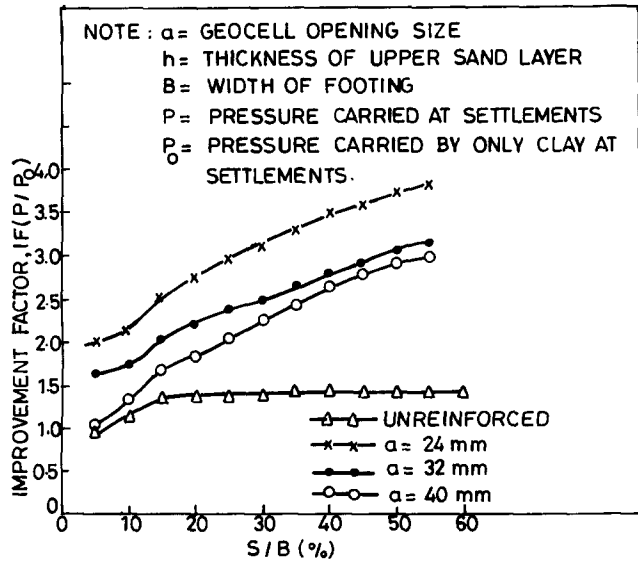


Figure 5 Variation of improvement factor with settlement ratio of  $h/B = 1.0$

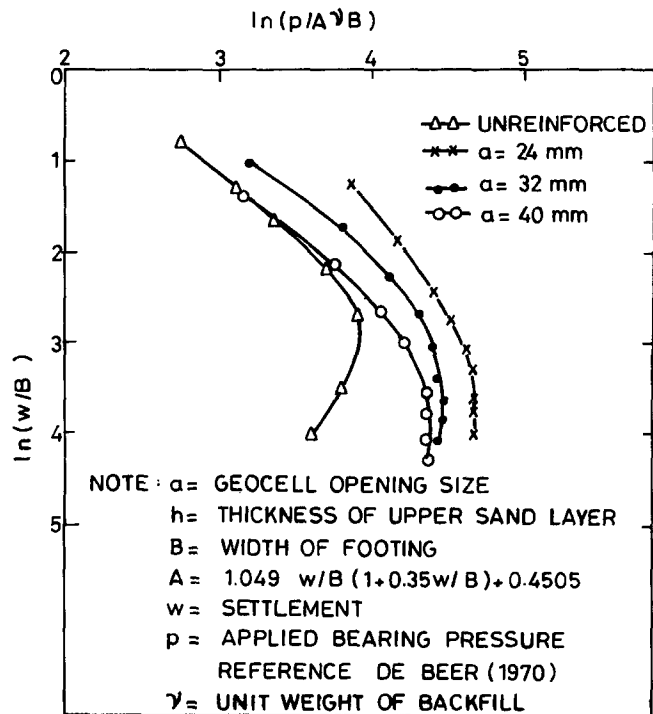


Figure 6 Evaluation of failure bearing pressure at  $h/B = 1.0$

Figure 6 shows the evaluation of average bearing pressure failure, i.e. bearing capacity and failure settlements for both unreinforced and reinforced sand by different geocell sizes at  $h/B = 1.0$ . The value of  $p/A\gamma B$  increases with increasing  $w/B$  and, at some point, it attains a maximum value beyond which it decreases with increasing  $w/B$ . The peak is treated as the failure point. It should be noted that the curves shift right and in an upward direction as the geocell size decreases. This plot gives the impression that, for a reduced geocell opening size, the failure pressure increases. But actually it can be seen that, after calculation of the failure pressure taking into consideration the failure settlement, we get a higher bear-

Table 6 Values of BCR and SRF at  $h/B = 1.0$

$h/B = 1.0$	BCR	SRF
Unreinforced	1.3	1.64
Reinforced:		
$a = 24 \text{ mm}$	3.4	3.0
$a = 32 \text{ mm}$	3.8	4.4
$a = 40 \text{ mm}$	4.2	5.3

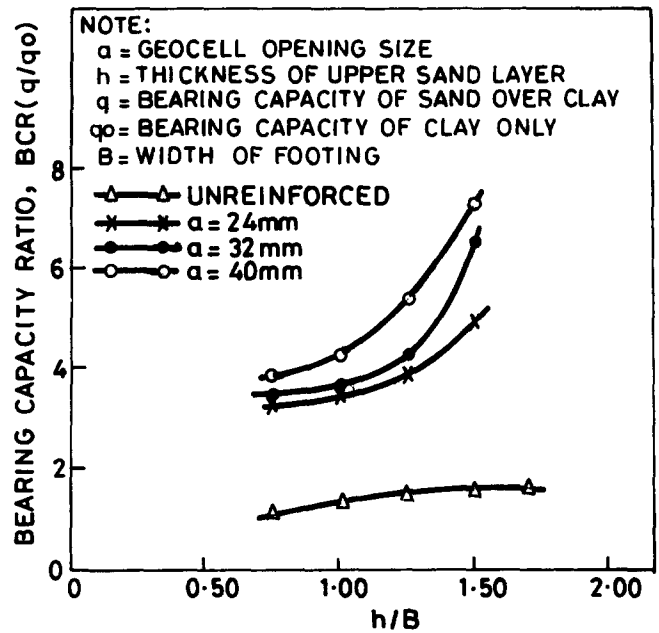


Figure 7 Relationship of bearing capacity ratio with  $h/B$  for unreinforced sand over soft marine clay

ing capacity for a larger geocell size. This anomaly could better be explained with reference to Figure 9. Table 6 shows the values of bearing capacity ratio (BCR) and settlement reduction factor (SRF) for  $h/B = 1.0$  for different geocell sizes and also for the unreinforced case.

Figure 7 shows the relationship between the bearing capacity ratio (BCR) and  $h/B$  for both the unreinforced and geocell-reinforced case with geocell opening sizes  $a$  of 24, 32 and 40 mm. In the unreinforced case BCR increases gradually with  $h/B$  and reaches a constant maximum value of 1.6 at  $h/B = 1.625$ .

Das<sup>6</sup> carried out studies on an unreinforced embedded strip footing and obtained a critical value of  $h/B$  of 1.5. For the surface footing a value of  $h/B$  higher than 1.5 in this case seems to be quite justified. There is no further increase of BCR with  $h/B$  as the failure wedges become fully confined in the sand layer. In the reinforced case there is a gradual increase of BCR at low value of  $h/B$  but there is a sharp increase of BCR after  $h/B = 1.25$ . From Figure 7 it can be seen that even at  $h/B = 1.5$  no peak value of BCR has been attained in any of the three curves for different geocell sizes. The beam action of the geocell structure in plane strain seems to be playing a certain role. An improvement of bearing capacity in the case of reinforced sand over unreinforced is evident from the figure. The bearing capacity at any thickness of sand layer is more in the case of a large geocell opening size.

Figure 8 shows the relationship between the settlement reduction factor (SRF) and  $h/B$  for both the unreinforced

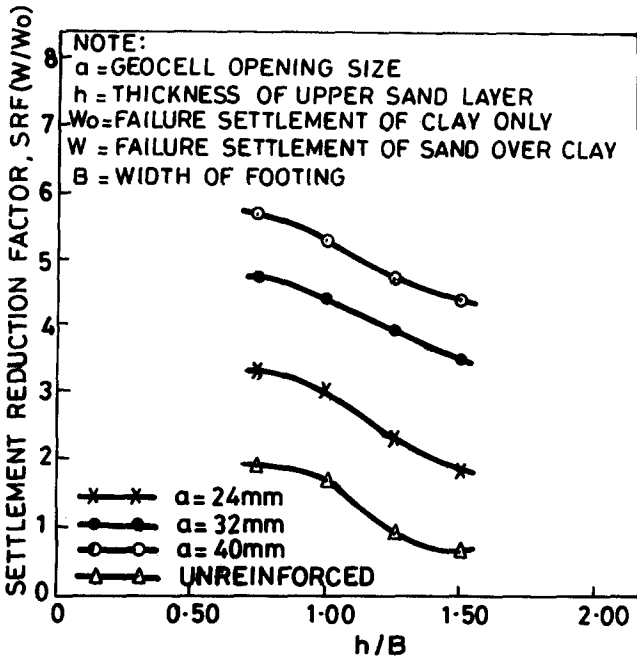


Figure 8 Variation of SRF with  $h/B$  for both unreinforced and geocell-reinforced cases

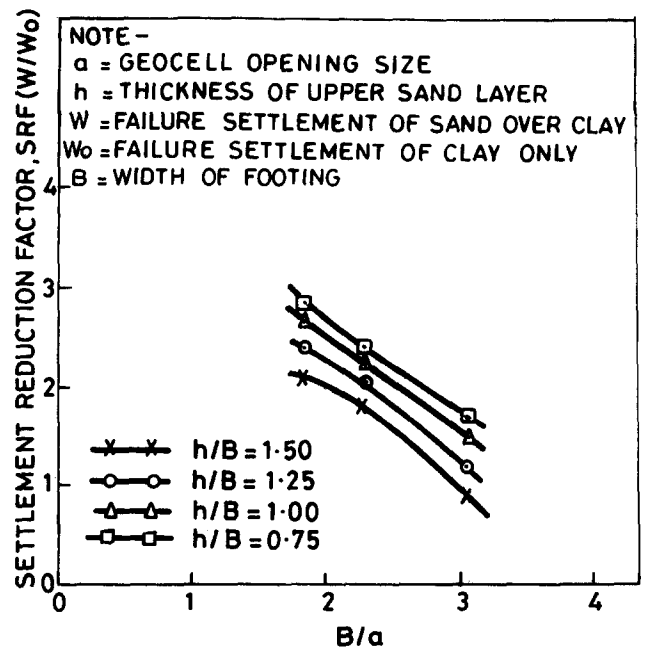


Figure 10 Relationship of settlement reduction ratio with  $B/a$  in geocell-reinforced sand over soft clay

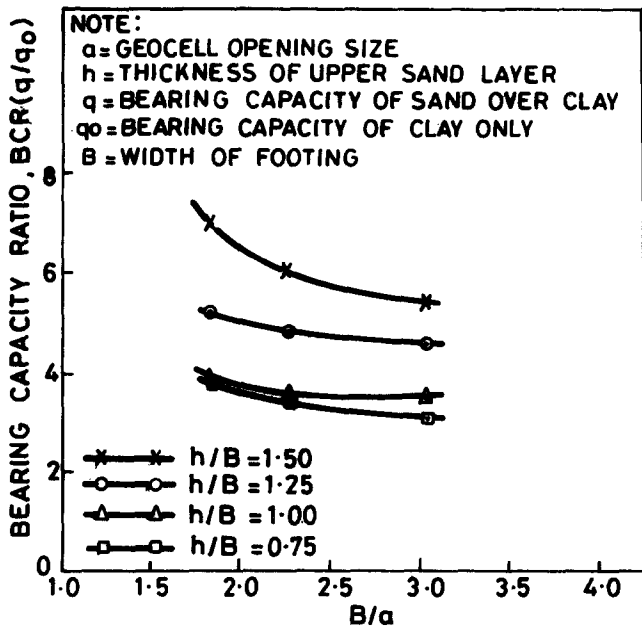


Figure 9 Relationship of bearing capacity ratio with  $B/a$  for reinforced sand over soft marine clay

and the geocell-reinforced case for three different cell sizes. In the unreinforced case, settlement reduction is negligible up to  $h/B = 0.75$  but then sharply decreases after  $h/B = 0.75$ . In the reinforced case there is a gradual decrease of settlement at failure with  $h/B$ . The shape of the curves changes from concave to convex after a certain thickness ratio. In the reinforced example settlement at failure is more than that in the unreinforced. It may be concluded from Figure 8 that, as the thickness of the layer increases, it becomes so stiff that it cannot bend and hence behaves just like a deep beam which fails only in vertical shear. At any thickness the settlement is more with the larger geocell size.

Figure 9 shows the relationship between BCR and  $B/a$  ( $B =$  width of footing,  $a =$  geocell size) for a geocell-reinforced sand layer at different thickness of layers, BCR increases with decreasing  $B/a$  for all the thicknesses of layers. There is a possibility of all curves reaching a peak value at  $B/a < 1.0$  if the same kind of plot given by Rea and Mitchell<sup>19</sup> for a paper cell is used. In other words it can be stated that as  $a$  increases BCR increases non-linearly, and it shows no trend of attaining a peak value of  $B/a$  of more than 1.5. Previously it was noted that load-settlement curves improve with use of a smaller geocell size. This anomalous behaviour can be explained as follows. As the geocell opening size increases the structure settles comparatively quicker under a particular pressure. As a result of excessive settlement the membrane action of the geocell walls starts to contribute to the bearing capacity. For smaller geocell sizes, failure occurs at lower settlement, i.e. before the commencement of membrane action, so for a larger size of geocell opening, an improved bearing capacity can be achieved at the cost of higher settlement. It should also be noted that for the purposes of a low-settlement (paved road) structure a smaller geocell size should be used, and for a large-settlement structure (unpaved road) a larger geocell size should be used to gain maximum benefit with respect to bearing capacity.

Figure 10 shows the variations of SRF with  $B/a$ . The SRF decreases with increasing  $B/a$ , i.e. decreasing  $a$ . So it may be concluded that, for a smaller geocell size, settlement is low because the compactness of the backfill material is more in the case of smaller geocell size. It should also be noted from Figure 10 that for a lower thickness of layer the curves flatten.

Figure 11 shows the variations of an improved bearing capacity factor ( $N_{\gamma}$ ) with  $h/B$  for different values of geocell opening size  $a$ . It can be seen from Figure 7 that, in the unreinforced case the maximum BCR is 1.6 at  $h/B = 1.625^6$  when the failure wedges are totally confined in the upper sand layer. This maximum constant value of

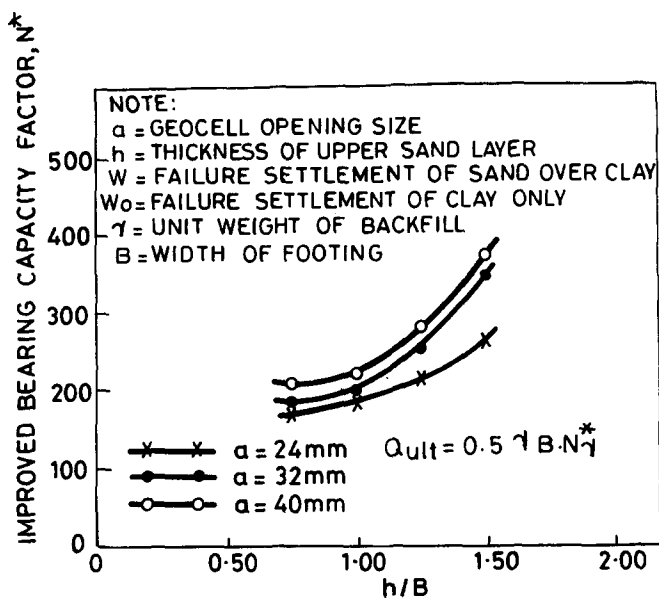


Figure 11 Variation of an improved bearing capacity factor for geocell-reinforced case with  $h/B$

bearing capacity is a function of the properties of the sand and is given by Meyerhof and Hanna<sup>20</sup> as  $q_s = 0.5\gamma BN_\gamma$ . Due to the use of the geocell layer, the bearing capacity of reinforced soil becomes much higher than the unreinforced value. The combined beam and membrane action of the geocell layer improves the bearing capacity and does not allow the failure wedges to touch the soft subgrade.

The average modified bearing capacity can be found by dividing the ultimate bearing pressure by  $0.5\gamma B$  ( $\gamma$  = unit weight of sand and  $B$  = footing width). The modified bearing capacity factor increases indefinitely with thickness of layer for every value of geocell size  $a$  as shown in Figure 11. This curve can be used for design purposes for small strip footings as geocell-reinforced sand over soft subgrade. Given the unit weight of backfill layer thickness and desired geocell opening size, the modified bearing capacity factor can be determined and, thus, the design bearing capacity can be found without resorting to experiment. The safe load can also be calculated.

## Conclusions

- 1 The stiffness of the upper elastic layer over soft marine clay increases with the thickness of the layer. The failure wedges in the unreinforced case are entirely confined in the sand layer at  $h/B = 1.625$  which closely tallies with the value obtained from the formulae given by Meyerhof and Hanna<sup>20</sup>.
- 2 The geocell layer exhibits a beam action up to a settlement ratio of 5–10%. After a settlement ratio of 20% the geocell layer exhibits a membrane action.
- 3 At large settlement the tensile strength of the geocell walls becomes important.
- 4 Load–settlement characteristics are improved by the use of geocell reinforcement.
- 5 An improvement of bearing capacity compared with the unreinforced example has been obtained at the

cost of increased settlement of the structure. As the settlement increases, bearing capacity also increases.

- 6 The low-settlement bearing capacity (i.e. at a settlement ratio of 10%) does not improve much compared to the unreinforced case, but the large-settlement bearing capacity (i.e. at a settlement ratio of 50%) shows considerable improvement.
- 7 The initial stiffness of the upper sand layer increases to a great extent because of the use of a geocell layer. Initial stiffness is greater in the case of the lower geocell opening size and increased geocell depth.
- 8 If the geocell opening size is more than at large settlement ratio, the geocell opening size does not affect the improvement factor.
- 9 The bearing capacity increases with increasing geocell opening size as well as the geocell thickness.
- 10 The settlement ratio increases with increasing geocell opening size but decreases with increasing geocell depth.
- 11 In order to get maximum benefit from geocell reinforcement, a smaller geocell opening size should be used in the case of a low-settlement structure (i.e. paved road) and a larger size can be used in the case of an unpaved road where large settlement is allowed.
- 12 Optimum values of geocell opening size and geocell depth cannot be obtained by such a small-scale experimental investigation because it is very difficult to work with larger geocell thicknesses as well as smaller geocell opening sizes.
- 13 An improved bearing capacity factor has been suggested which gives a total improvement in bearing capacity at any geocell opening size and depth.

## Acknowledgements

The authors are grateful to Professor B. Nag, Director, Indian Institute of Technology, Bombay, for his encouragement and the use of facilities.

## References

- 1 Binquet, J. and Lee, L.L. Bearing capacity analysis of reinforced earth slab. *J Geotech. Eng. Div., ASCE* 1975, **110**, GT 12, 1257–1275
- 2 Ingold, T.S. and Miller, K.S. The behaviour of geotextile reinforced clay subjects to undrained loading. *2nd Int. Conf. on Geotextiles, Las Vegas, USA*, 1982, pp.593–597
- 3 Fragazy, R.J. and Lawton, E. Bearing capacity of reinforced sand subgrade. *J. Geotech. Eng. Div., ASCE* 1984, **101**, GT 10, 1500–1507
- 4 Guido, V.A., Sobiech, J.P. and Christon, S.N. A comparison of texturised and nontexturised geoweb reinforced earth slabs. *Geosynthetic-1989 Conf., San Diego, USA*, 1989, pp.215–230
- 5 Love, J.P., Burd, H.J., Milligan, G.W.E. and Houslyby, G.T. Analytical and model studies of reinforcement of a layer of granular fill on a soft clay subgrade. *Can. Geotech. J.* 1987, **24**, 611–622
- 6 Das, B.M. Foundation on sand underlain by soft clay with geotextile at sand–clay interface. *Geosynthetic-89 Conf., San Diego, USA*, 1989, pp.203–213
- 7 Madhav, M.R. Analysis of settlement of geotextile reinforced soil. *Proc. Workshop on Application Potential of Geosynthetics in Civil Engineering, CBRI, Roorkee, India*, 1989, pp.131–143
- 8 McGown, A., Andrawes, K.Z. and Kabir, M.H. Load extension testing on geotextiles confined in soil. *Proc. 2nd Int. Conf. on Geotextiles, Las Vegas, USA*, 1982, pp.793–804

- 9 Mandal, J.N. and Sah, H.S. Bearing capacity tests on geogrid-reinforced clay. *Int. J. Geotext. Geomembranes* 1992, **11**, 327-333
- 10 Garidel, D.R. and Morel, G. New soil strengthening techniques by textile element for low volume roads. *Proc. 3rd Int. Conf. on Geotextiles, Vienna, Austria*, 1986, pp.1027-1032
- 11 Khay, M. and Perrier, H. Sand confinement by geotextiles in road construction. *4th Int. Conf. on Geotextiles, Geomembranes and other Related Products*, 1990, p.255
- 12 Kazerani, B. and Jamnejad, G.H. Polymer grid cell reinforcement in construction of pavement structure. *Geosynthetic* 87, 1987, Vol. 1, pp.58-68
- 13 Basett, D. General discussion by M.D. Bolton. *Proc. Conf. in Reinforced Embankments, theory and practice in the British Isles, Cambridge University, UK*, 1989, pp.169-177
- 14 Mhasikar, S.Y. and Mandal, J.N. Soft clay subgrade stabilization using geocells. *Proc. ASCE, Speciality Conf., Grouting, Soil Improvement and Geosynthetics, New Orleans, USA*, 1992, Vol. 2, pp.1092-1103
- 15 Paul, J. Reinforced soil systems in embankment construction practices. *Proc. Int. Geotechnical Symp. on Theory and Practice of Earth Reinforcement, Japan*, 1988, pp. 461-466
- 16 Shimizu, M. and Inui, T. Increase in the bearing capacity of ground with geotextiles wall frame. *4th Int. Conf. on Geotextiles, Geomembranes and other Related Products, The Netherlands*, 1990, p.254
- 17 Bush, D.I. Jenner, C.J. and Bassett, R.H. The design and construction of a geocell foundation mattress supporting embankment. *Int. Geotechnical Symp. on Theory and Practice of Earth Reinforcement, Fukuoka, Japan*, 1988, pp.209-214
- 18 De Beer, E.E. Experimental determination of the shape factors and the bearing capacity factors of sand. *Geotechnique* 1970, **20**, 387-411
- 19 Rea, G. and Mitchell, J. Sand reinforcement using paper grid cells. *Int. Symp. on Earth Reinforcement, Pittsburgh, USA*, 1978, pp.644-662
- 20 Meyerhof, G.G. and Hanna, A.M. Ultimate bearing capacity of footing on sand layer overlying clay. *Can. Geotech. J.* 1974, **11**, 223-229